

Unambiguous phase-shift analysis of the  $^{12}\text{C}(^{12}\text{C},\alpha)^{20}\text{Ne}$  reaction at Coulomb-barrier energies

Z. Basrak

*Rudjer Bošković Institute, 41001 Zagreb, Yugoslavia**and Physikalisches Institut der Universität Erlangen-Nürnberg, 8520 Erlangen, Federal Republic of Germany*

W. Tiereth, N. Bischof, H. Fröhlich, B. Nees, E. Nieschler, and H. Voit

*Physikalisches Institut der Universität Erlangen-Nürnberg, 8520 Erlangen, Federal Republic of Germany*

(Received 2 January 1985)

Excitation functions of the reaction  $^{12}\text{C}(^{12}\text{C},\alpha)^{20}\text{Ne}$  have been measured in energy steps of 25 and 12.5 keV from  $E_{c.m.} = 5.7$  to 6.1 MeV at 18 angles between  $\theta_{c.m.} = 5^\circ$  and  $90^\circ$ . A recently published method for the determination of the true  $S$ -matrix elements of a reaction including only spinless particles was applied to the  $\alpha_0$  exit channel. All quasimolecular resonances previously reported in the energy range studied were confirmed and spin assignments are made.

## I. INTRODUCTION

A recent investigation of the  $^{12}\text{C} + ^{12}\text{C}$  total reaction cross section<sup>1</sup> in the vicinity of the Coulomb barrier revealed the existence of additional resonances of the quasimolecular-type not yet clearly identified in the  $\alpha$ -particle exit channel. In order to verify whether all the resonances observed in the total reaction cross section can be identified in the  $\alpha$ -particle exit channel and, if so, to determine the spin of the resonances, we remeasured the  $^{12}\text{C}(^{12}\text{C},\alpha)^{20}\text{Ne}$  reaction.

The  $^{12}\text{C} + ^{12}\text{C}$  system is well known for its strongly fluctuating excitation functions and angular distributions. The shape of the angular distributions of the  $\alpha$ -particle exit channels, which incorporate the main part of the reaction flux at Coulomb barrier energies, changes very drastically within small energy intervals. If resonance spins are to be determined, it is, therefore, of great importance to use angular distributions measured as closely as possible to the true resonant energy. It is impossible to measure just at the energies where resonances are reported, since these values are subject to the energy calibration of the accelerator and the energy loss of the projectiles in the target. For the case of overlapping resonances it is, moreover, necessary to follow the contribution of the particular partial wave with energy.

To apply a recently published<sup>2,3</sup> method for the determination of the true  $S$ -matrix elements of a reaction involving only zero-spin particles, it is also important to follow the energy dependence of the  $S$ -matrix elements in small energy steps. We have, therefore, performed a high-resolution study of the  $^{12}\text{C} + ^{12}\text{C}$  system at the Coulomb barrier with emphasis on the  $\alpha_0 + \text{Ne}$  exit channel. For this purpose we used a very thin, windowless gas target, small energy steps, and the simultaneous detection of the reaction products at 21 angles with reasonably good counting statistics.

## II. EXPERIMENTAL METHODS

The measurements were performed at the University of Erlangen EN tandem accelerator in the energy range

$E_{c.m.} = 5.69\text{--}6.11$  MeV in steps of 25 keV (c.m.) and 12.5 keV for a few selected regions. Angular distributions for the  $\alpha$ -particle exit channels of the  $^{12}\text{C} + ^{12}\text{C}$  collision have been measured simultaneously for each energy at 21 angles equally spaced in the angular range from  $4^\circ$  to  $73^\circ$  (lab) corresponding to  $\theta_{c.m.} \approx 5.3^\circ\text{--}91.7^\circ$ . (The angular distributions are symmetric about  $90^\circ$  due to the identity of the nuclei in the entrance channel.) For this purpose a multidetector array was used in which detectors were mounted in  $7^\circ$  steps left and right with respect to the beam direction.

With intent to improve the counting rate without deteriorating the angular resolution (for a fixed detector-target distance), large solid angles were achieved using rectangular-shaped surface-barrier detectors ( $30 \times 5$  mm nominal detector surface). To minimize, for a given solid angle, the acceptance of the detectors with respect to the polar angle we used slits in front of the detectors with optimized width and height ratios. The largest solid angle was 5.3 msr, the greatest angular spread  $2.2^\circ$  (lab). Occasionally, some of the detectors did not work properly. In any case, at least 18 angles have been measured simultaneously for each angular distribution.

To distinguish  $\alpha$  particles from other light reaction products, appropriate depletion depths for the detectors have been used. Al foils in front of the detectors served to stop all heavy reaction products.

The  $^{12}\text{C}$  beam was focused through a slit of 2 mm in diameter placed in front of a small Faraday cup which was mounted closely behind the target. The slit was connected to a galvanometer. The stability of the experiment was continuously controlled by three monitor detectors placed at  $17^\circ$ ,  $24^\circ$ , and  $45^\circ$  (lab).

A windowless, differentially pumped gas target<sup>4</sup> was used. The gas was commercially available propane,  $\text{C}_3\text{H}_8$ . It was flowing into the target area through a 0.3 mm nozzle of the Laval-type with an initial pressure of 2.6 atm. The gas pressure was permanently monitored so that the target thickness was perfectly stable in time. The target thickness was determined from an energy loss<sup>5</sup> measurement with a low intensity ( $10^3$  particles per second) 9 MeV (lab) oxygen beam which could be easily produced

by means of the two  $90^\circ$  analyzing magnets installed at the accelerator: Since the heavy-ion beam transmitted by the first magnet in a definite charge state  $q$  is the subject to charge changing processes in the rest gas between the two magnets, the second magnet can be used to select a charge state  $q' \neq q$  with the low intensity necessary. The  $^{12}\text{C}$  portion of the target was  $2.0 \pm 0.5 \mu\text{g cm}^{-2}$ . Target impurities other than hydrogen were negligible. The total target thickness was equivalent to an energy loss of about 25 keV (lab) for the incoming  $^{12}\text{C}$  ions.<sup>5</sup> All energies stated in the figures and quoted in the text are corrected for this energy loss.

Normalization of the data was achieved using a Faraday cup and monitor detectors as well as earlier measurements performed in the same energy range.<sup>6</sup> From the errors involved in the above procedure we estimate the deduced energies to be accurate within  $\pm 10$  keV, while the relative cross section has an error of  $\pm 10\%$  at the most.

### III. EXPERIMENTAL RESULTS AND ANALYSIS

A simple method for the determination of the true  $S$ -matrix elements (i.e., the contribution of every partial wave to the cross section) of a two-body reaction involving only spinless particles has been recently proposed.<sup>2,3</sup> For such a reaction all the information concerning the reaction dynamics (no polarization effects) is contained in measured angular distributions. We will briefly sketch the essentials of this analysis in the following.

The set of the discrete data points  $\sigma(\theta_i)$  with errors

$\Delta\sigma(\theta_i)$  is replaced by the continuous best-fit curve chosen in the form of a polynomial in  $x = \cos\theta$  of degree  $2L$  with real coefficients where  $L$  accounts for the highest contributing partial wave

$$\{\sigma(\theta_i), \Delta\sigma(\theta_i)\} \rightarrow \sigma(x) = \sum_{l \text{ even}}^{2L} A_l x^l = \sum_{l \text{ even}}^{2L} a_l P_l(x), \quad (1)$$

where  $P_l(x)$  is the Legendre polynomial of degree  $l$ . The polynomial  $\sigma(x)$  can be expressed in the factorized form

$$\sigma(x) = A_{2L} \prod_{i=1}^L (x - z_i)(x - z_i^*) = \left| \sqrt{A_{2L}} \prod_{i=1}^L (x - z_i) \right|^2 = |F(x)|^2, \quad (2)$$

where  $z_i$  are zeros of the associated equation  $\sigma(x) = 0$ . The asterisk stands for complex conjugation. After a straightforward reorganization of the coefficients, the reaction amplitude  $F(x)$  can be brought into the standard form

$$F(x) = \sum_{l=0}^L b_l P_l(x) = \frac{1}{2ik} \sum_{l=0}^L (2l+1) S_l P_l(x), \quad (3)$$

where  $k$  is the entrance channel wave number and

$$S_l = |S_l| \exp(2i\delta_l)$$

is the  $S$ -matrix element associated to the  $l$ th partial wave.

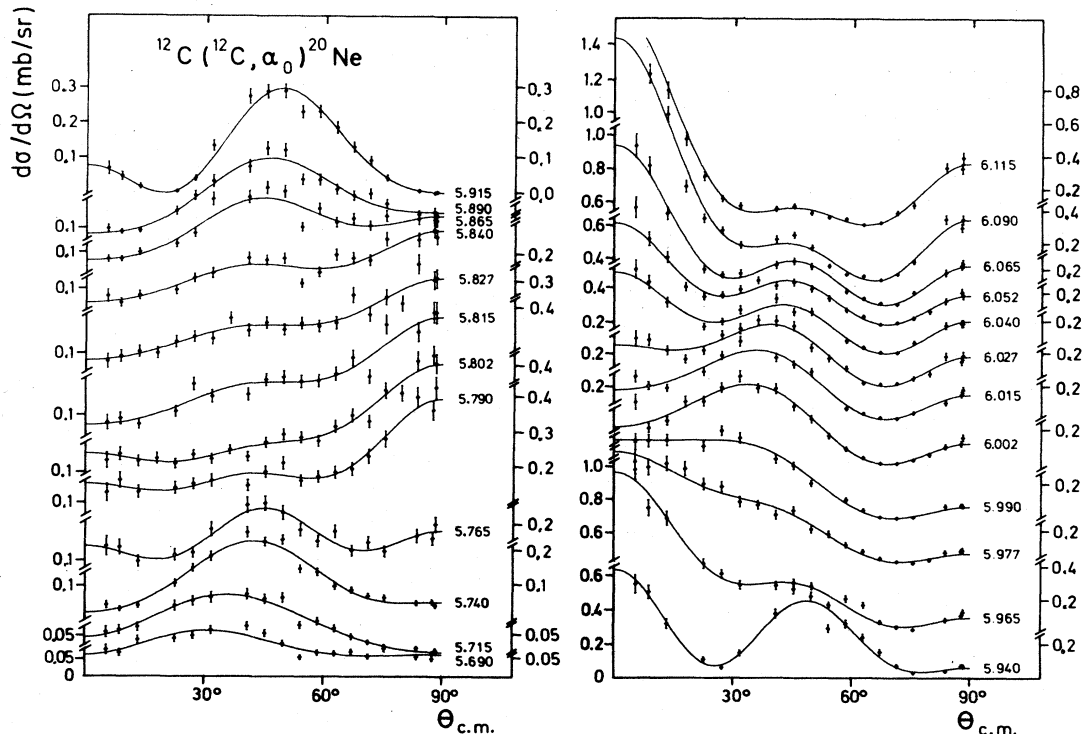


FIG. 1. Angular distributions of the reaction  $^{12}\text{C}(^{12}\text{C}, \alpha_0)^{20}\text{Ne}$ . The numbers at the right indicate the c.m. energy at which the corresponding angular distribution has been measured. The solid curves are the results of a  $\chi^2$  fit to the data using Eq. (1) with  $2L = 8$ .

It can be shown that, for a given  $L$ , only one set of linear expansion coefficients  $a_l$  gives the best fit of the measured cross section and that there are, generally,  $2^L$  different sets of coefficients  $b_l$  which are all mathematically equivalent in the sense that all of them give exactly the same function  $\sigma(x)$  when substituted into (3) and (2) (see Ref. 3 and references therein). A given set of coefficients  $b_l$  [i.e.,  $S$ -matrix elements  $S_l = 2ik(2l+1)^{-1}b_l$ ] determines a particular reaction amplitude  $F(x)$ . Thus, one obtains a  $2^L$ -fold solution<sup>7</sup> of the reaction problem. In addition, the phase of the reaction amplitude  $F(x)$  is arbitrary.

The chosen set of  $L$  (out of  $2L$ ) zeros determines one particular solution  $F(x)$ . The solutions can be formally distinguished and ordered by means of that set of zeros which is used to generate them.<sup>8</sup> In case of a reaction with identical particles in the entrance channel only even partial waves can contribute in the sum of Eq. (3). Furthermore, the zeros of Eq. (2) are grouped on circles around the origin of the complex  $x$  plane. On each circle there are four zeros symmetrically positioned with respect to the coordinate axes. From each quadruplet only the two zeros which are symmetric with respect to the origin of the complex  $x$  plane generate an amplitude  $F(x)$  in accordance with reaction symmetry. Therefore, the number of different reaction amplitudes cannot exceed  $2^{L/2}$ . It follows, also, that modulus  $|b_l|$  (or  $|S_l|$ ) has half the ambiguity of  $b_l$  (or  $S_l$ ) itself.

Figure 1 shows the 24 measured angular distributions for the transition to the  $J^\pi = 0^+$  ground state of the residual nucleus  $^{20}\text{Ne}$ . The error bars include the error from the counting statistics only. Curves drawn through the data points are the result of a  $\chi^2$  best fit to the measured angular distributions using expansion (1) with  $2L = 8$ . The  $\chi^2$  value obtained is typically 1.3; it exceeds 1.6 only in case of five angular distributions.

Inclusion of the next higher partial wave ( $l = 6$ ) in the probe function  $\sigma(x)$  (with  $2L = 12$ ) improved the  $\chi^2$  value by about 30% at the most. It is important to note that the inclusion of the  $l = 6$  partial wave did not always improve the fit in those cases where a  $\chi^2$  value larger than 1.6 was obtained before. This shows that the quality of the data, rather than missing partial waves, results in somewhat higher  $\chi^2$  values. (Inclusion of the partial waves  $l \geq 8$  is not justified in this energy region.)

Figure 2 displays the energy dependence of the expansion coefficients  $a_l$  (filled circles). Open circles denote  $a_l$  values obtained from a fit of the data of Ref. 6. The measurements of Ref. 6 have been performed with larger energy steps (50 keV) and considerably thicker solid  $^{12}\text{C}$  targets ( $8\text{--}15 \mu\text{g cm}^{-2}$ ). The overall agreement between the present and the previous<sup>6</sup> data is very good, though, as a result of the better energy resolution, the behavior of the coefficients  $a_l$  from the present investigation can be taken with much higher confidence; the energy dependence is much smoother, and there exist no jumps between adjacent points. The largest discrepancy between previous and present data shows up at 5.94 MeV and is probably due to an incorrect point in the old data which is known to be remeasured with experimental conditions different from those of the adjacent data points. This discrepancy does,

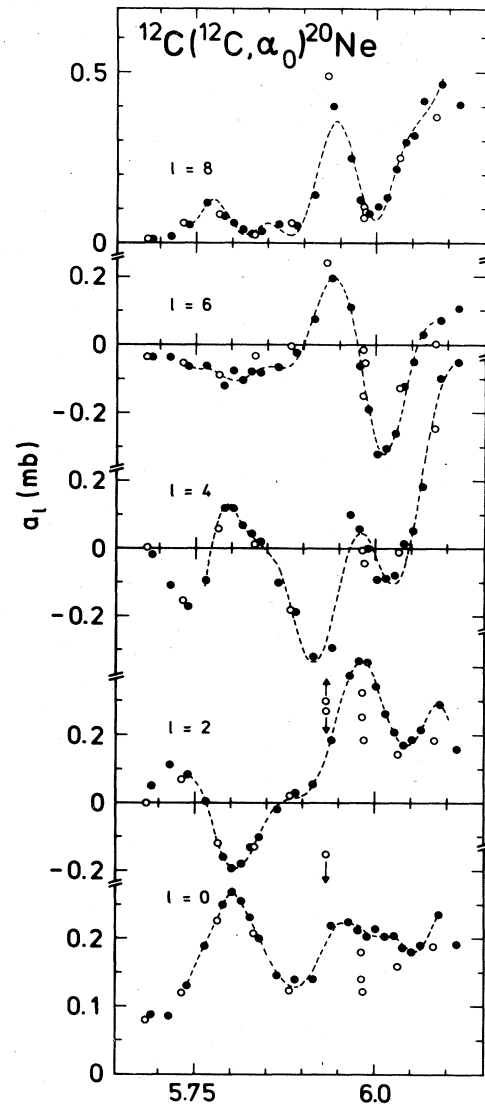


FIG. 2. Energy dependence of the expansion coefficients  $a_l$  of the fit curves shown in Fig. 1 (filled circles). The open circles show  $a_l$  values obtained from an analysis of the data of Ref. 6. The dashed curves are polynomial fits to the filled circles.

however, not alter the conclusions drawn in Ref. 6 mainly from the summed cross section (first six transitions to  $^{20}\text{Ne}$ ), nor does it cast doubt on the existence of the resonance at 5.94 MeV.

It is interesting to note that the present investigation does not reveal finer structures than observed in Ref. 6 even though much higher resolution was used. This is particularly obvious from the energy dependence of the  $a_0$  values which are proportional to the angle integrated cross section.

There exist four ( $2^{L/2}$ , identical particles) different reaction amplitudes for any angular distribution since acceptable fits to the data could be obtained with partial waves  $l = 0, 2$ , and  $4$  (i.e., with  $2L = 8$ ). Only one of these represents the true physical solution.<sup>2,3</sup> There is, however,

no physical criterion to eliminate any one of the solutions at one particular energy. The criterion most widely used to distinguish between different solutions is a continuity criterion. One can impose this criterion on the energy dependence of the  $S$ -matrix elements (i.e., smoothness condition) or/and on the trajectories which connect zeros at consecutive energies in the complex  $x$  plane.<sup>2,3</sup>

If one particular partial wave resonates, the corresponding  $S$ -matrix element describes a loop in the Argand diagram. Unfortunately, no similar rule for the trajectories connecting adjacent zeros exists.

In Ref. 3 a procedure has been worked out to obtain a set of  $b_l$  values (with fixed  $l$ ) which belong together in the energy range considered, i.e., a procedure to connect the solutions at adjacent energies ("three-point"—shortest-path method). This procedure did not give unambiguous results in the present case since a degeneration of solutions exists for a few energies. This degeneration is a consequence of double zeros ( $z_i^* = z_i$ ).

In contrast to the coefficients  $b_l$  of relation (3), which are subject to ambiguities, the set of zeros  $z_i$  is a unique feature of the polynomial function  $\sigma(x)$  and, thus, of the measured angular distribution. That is why we turn in the following to the zeros in order to establish a connection between solutions which belong together at adjacent energies. According to Ref. 9 we generated a smooth function for the expansion coefficients  $a_l$  by fitting them with a polynomial function (dashed curve in Fig. 2). With this analytical representation of the coefficients  $a_l$  one is able to calculate zeros in very fine energy steps and to reconstruct the zero trajectories with the desired precision. The obtained continuous zero trajectories (solid curves in Fig. 3) give us the unambiguous evolution of the zeros determined for the measured angular distributions (circles in Fig. 3; they are connected with dashed lines whenever misinterpretation could occur) with increasing energy. For the sake of clarity only one pair of the zero trajectories, out of the two possible pairs, is shown in Fig. 3. The choice of another combination of zeros (i.e., of another starting solution of the reaction amplitude) would give a pattern similar to that of Fig. 3: One or both of the zero trajectories would be replaced by its mirror image with

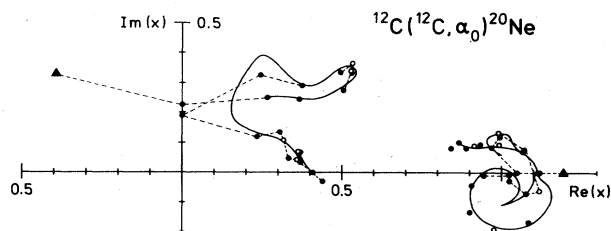


FIG. 3. Zeros of the reaction amplitude  $F(x)$ ,  $x = \cos\theta$ . Solid curves represent the analytic simulation of the actual measurement (dashed curve in Fig. 2), while dashed lines join the zeros (filled and open circles), resulting from the analysis of the experimental angular distributions, whenever a misinterpretation could occur. Open circles stand for zeros which correspond to the angular distributions measured in 12.5 keV steps. Zeros of the smallest energy are labeled by a triangle. For further explanations see the text.

respect to the real axis (complex conjugation). These four combinations give all possible reaction amplitudes (identical nuclei). It has been mentioned above that these different solutions  $F(x)$  are mutually complex conjugates. It can be shown<sup>3</sup> that the causality condition can be used in case of a resonance in order to determine which of the two complex conjugate solutions is the physical one: The loop in the Argand diagram has to evolve counterclockwise with increasing energy.

Since the reaction amplitude  $F(x)$ , and, therefore, also the  $S$ -matrix elements, have arbitrary overall phase, which cannot be determined in an energy independent analysis, we plot in Fig. 4 the energy dependence of the moduli  $|S_l|$  of the  $S$ -matrix elements weighted by  $(2l+1)^{1/2}$ . The solution represented by filled circles (solution I) corresponds to the choice of zeros shown in Fig. 3. Solution II (open circles in Fig. 4) represents the other possible solution which is obtained if one of the two zero trajectories of Fig. 3 is replaced by its complex conjugate counterpart (the amplitude of the highest partial wave is unique<sup>3,8</sup>).

The continuity condition, assumed to be valid for zeros, requires that the modulus of the physical solution either follows the set of solutions represented by open or the one

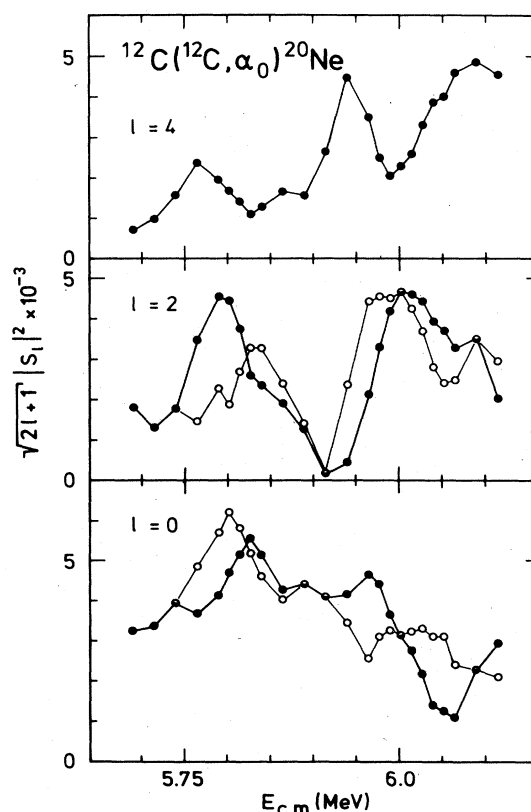


FIG. 4. Absolute values of  $S$ -matrix elements multiplied by  $(2l+1)^{1/2}$  as a function of energy. These quantities are proportional to the partial reaction cross sections  $\sigma_l = 2\pi k^{-2}(2l+1)|S_l|^2$ . Filled circles correspond to the solution generated by the zeros of Fig. 3 and open circles to the other possible solution (see the text). The lines connecting the points are intended to guide the eye.

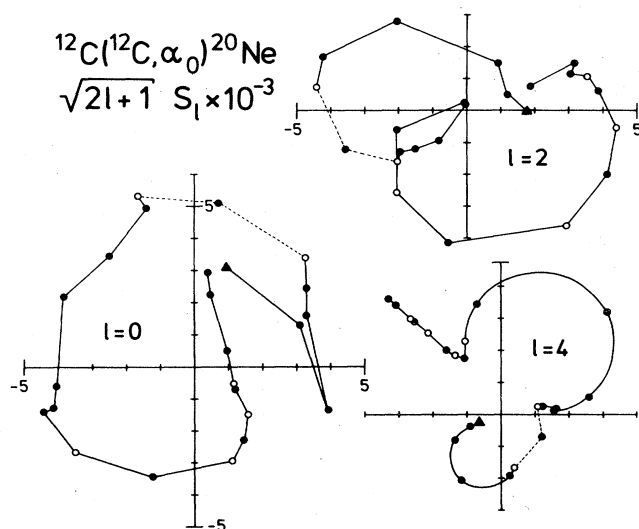


FIG. 5. Argand diagrams for the  $l=0$ , 2, and 4 partial waves. The meaning of the symbols is the same as in Fig. 3. The broken lines are intended to guide the eye. The loops in the  $l=4$  plot are the result of a Breit-Wigner fit. For further information see the text.

represented by filled circles and that they cannot be interchanged at any energy. These two solutions are very similar, and, if an energy-independent phase-shift analysis is to be performed, only experiments at very low energies could possibly reveal which set is the physical one. An energy-dependent analysis, in which the energy behavior of the  $S$ -matrix element is to be described through some model, can, however, be useful in determining the unique (physical) solution in a limited energy region.

Since the  $S$ -matrix element of the highest contributing partial wave has the unambiguous modulus we chose the  $|S_4|$ -excitation function and performed a fit in the energy range 5.69–6.00 MeV (c.m.) with a coherent sum of two Breit-Wigner-type resonances. In this way, the overall phase of the  $S$ -matrix can be fixed from energy to energy for the entire energy range studied and the Argand diagrams for all  $l$  values can be plotted. (The  $S$ -matrix phase is still free at the smallest energy.)

Solution II results in erratical Argand diagrams. Moreover, the loops for different  $l$  values move in opposite directions, which is physically inadmissible. On the other hand, solution I behaves very regularly with energy (see Fig. 5). The loops for  $l=0$  and 2 move counterclockwise, as demanded by the causality condition. Therefore, we conclude that solution I represents the physical solution and gives the true  $S$  matrix in the energy interval studied. It should be noted that the whole  $S$  matrix was turned by

+45° at 5.81 MeV, and for all subsequent energies (5.83 MeV and higher) by +90°. (These points are connected by dashed lines in Fig. 5.) This procedure did not alter the main feature of the two Breit-Wigner circles in the  $l=4$  Argand diagram (cf. Fig. 5).

The  $l=0$  partial reaction amplitude seems to be either composed of several narrow resonances or is the result of an interference between a resonance and a slowly varying background. To clarify this point the measurements have to be continued to lower energies.

#### IV. DISCUSSION

Figure 4 shows that the absolute values of the  $S$ -matrix elements  $|S_l|$  exhibit quite a few pronounced structures within the small energy range investigated (400 keV). These structures are concentrated at the c.m. energies 5.8, 5.94, and 6.0 MeV, where also the angle integrated cross section for the  $\alpha_0$  exit channel shows structures (see the  $\alpha_0$  excitation function of Fig. 2) known from previous investigations to be real quasimolecular resonances.<sup>1,6</sup> Both sets of solutions happen to have a very similar energy dependence (particularly in case of  $l=2$ ) with a small shift (10–30 keV) in the location of corresponding maxima.

If we assume that solution I represents the physical reality we find the resonance energies  $E_R$ , resonance widths  $\Gamma_R$ , and  $J^\pi$  values listed in Table I. Obviously, the resonance with  $E_R \approx 5.8$  MeV showing up in the integrated  $\alpha_0$  cross section (Fig. 2) and in the total reaction cross section<sup>1</sup> is a resonance triplet with  $J^\pi$  values  $4^+$ ,  $2^+$ , and  $0^+$ . The  $0^+$  component has been identified already in Ref. 10. Only the resonance at 5.94 MeV which has been found in different exit channels ( $\alpha$ -particle exit channel,<sup>6,11</sup>  $^8\text{Be}$  exit channel,<sup>12</sup> total reaction cross section<sup>1</sup>) seems to be a single resonance with a  $J^\pi$  value of  $4^+$ . The resonance at  $E_R \approx 6.0$  MeV showing up in the  $\alpha_0$  cross section of this work and in the total reaction cross section<sup>1</sup> seems to be a resonance doublet with  $J^\pi$  values  $0^+$  and  $2^+$ . It is interesting to note that a resonance has been found at 6.0 MeV in the carbon-carbon radiative capture<sup>13</sup> having a  $J^\pi$  value consistent with  $2^+$ .

In summary, we applied a new approach for a reaction phase-shift analysis (only spin 0 particles) to carefully measured high resolution data. The analysis confirmed the existence of resonance structures known to exist in the energy range studied. It was able to resolve two of these structures and to determine the resonance spins. We believe that the energy-dependent analysis carried out in this work gives the truly unique (the “physical”) solution of the reaction problem.

TABLE I. Resonance energies  $E_R$ , resonance widths  $\Gamma_R$ , and  $J^\pi$  values for resonances deduced from the  $|S_l|$  plots of Fig. 4. In case of  $l=0$  and 2 solution I was used.

$E_R$ (MeV)	5.77	5.80	5.82	5.94	(5.97)	6.01
$\Gamma_R$ (keV)	60	60	50	50	(50)	70
$J^\pi$	$4^+$	$2^+$	$0^+$	$4^+$	$0^+$	$2^+$

This work was supported in part by the Deutsche Forschungsgemeinschaft, Bonn, Federal Republic of Germany; by the Internationales Büro der Kernforschungsan-

lage Jülich, Jülich, Federal Republic of Germany; and by the Scientific Community of the Republic of Croatia, Zagreb, Yugoslavia.

- 
- <sup>1</sup>W. Treu, H. Fröhlich, W. Galster, P. Dück, and H. Voit, *Phys. Rev. C* **22**, 2462 (1980).
- <sup>2</sup>Z. Basrak, F. Auger, P. Charles, W. Tiereth, and H. Voit, *Lecture Notes in Physics 211*, edited by S. Albeverio, L. S. Ferreira, and L. Streit (Springer, Berlin, 1984), p. 347.
- <sup>3</sup>Z. Basrak and F. Auger, *Nucl. Phys. A* **441**, 150 (1985).
- <sup>4</sup>G. Bittner, W. Kretschmer, and W. Schuster, *Nucl. Instrum. Methods* **167**, 1 (1979).
- <sup>5</sup>L. C. Northcliffe and R. F. Schilling, *Nucl. Data, Sect. A*, **A7**, 233 (1970).
- <sup>6</sup>W. Galster, W. Treu, P. Dück, H. Fröhlich, and H. Voit, *Phys. Rev. C* **15**, 950 (1977).
- <sup>7</sup>N. P. Klepikov, *Zh. Eksp. Teor. Fiz.* **41**, 1187 (1961) [*Sov. Phys.—JETP* **14**, 846 (1962)].
- <sup>8</sup>Z. Basrak (unpublished).
- <sup>9</sup>A. de Bellefon and A. Berthon, *Nucl. Phys.* **B109**, 129 (1976).
- <sup>10</sup>F. Coçu, J. Uzureau, S. Plattard, J. M. Fieni, A. Michaudon, G. A. Keyworth, M. Cates, and N. Cindro, *J. Phys. (Paris) Lett.* **38**, L421 (1977).
- <sup>11</sup>E. Almqvist, D. A. Bromley, and J. A. Kuehner, *Phys. Rev. Lett.* **4**, 515 (1960).
- <sup>12</sup>R. Wada, J. Shimizu, and K. Takimoto, *Phys. Rev. Lett.* **38**, 1341 (1977).
- <sup>13</sup>A. M. Sandorfi and A. M. Nathan, *Phys. Rev. Lett.* **40**, 1252 (1978).